Exploring the relationship between cocrystal stability and symmetry: is Wallach's rule applicable to multi-component solids?†

Tomislav Friščić,[a] László Fábián,[b] Jonathan C. Burley,[c] David G. Reid,[d] Melinda J. Duer[d] and William Jones*[a]

Received (in Cambridge, UK) 13th November 2007, Accepted 4th January 2008
First published as an Advance Article on the web 30th January 2008
DOI: 10.1039/b717532a

Comparison of structure and hydration stability of pairs of chiral and racemic binary cocrystals indicates that the racemic solid is more stable than the chiral one; we illustrate that this difference might arise from intermolecular (crystal packing) factors in one case, while intramolecular (molecular conformation) factors are more significant in the other.

Recent years have witnessed a rapid growth of interest in multi-component crystals (cocrystals)[1,2] as functional solid-state materials.[3–5] Whereas it has been established that a particular cocrystal former can bring about a significant enhancement of a solid-state property,[6] the selection of co-crystal components is still largely a matter of trial-and-error rather than design.[7] With our interest in constructing cocrystals as pharmaceutical and functional materials, we have recently begun exploring general rules connecting the physicochemical properties of cocrystals to their crystal and molecular structures. In that context, we decided to address the effect of symmetry on the stability of cocrystals.[8] Our interest in symmetry was motivated in part by an empirical rule related to single-component molecular crystals. According to the so-called Wallach's rule, a racemic crystal is expected to have a higher density than its chiral counterpart.[9] As a result of more efficient packing, the overall stability of the crystal is anticipated to follow the same trend. To establish whether such a rule would exist for cocrystals, we decided to contrast the physicochemical properties of chiral and racemic forms of cocrystals[10] based on the model APIs theophylline (**tp**) and caffeine (**caf**) (Scheme 1).[11]

Pairs[12] of racemic and chiral cocrystals were obtained by combining the model APIs with racemic and chiral forms of tartaric (D- and DL-**ta**) and malic acids (D- and DL-**ma**).‡ We were particularly interested in observing possible differences in a pharmaceutically important[13] physicochemical property: stability towards hydration.§ Cocrystallisation from solution did not provide cocrystals with either D- or DL-**ma**, and we turned to liquid-assisted grinding as a more efficient synthetic method, which was previously used to obtain cocrystals of **tp** and **caf** with **ta**.[11,14]

Synthesis by liquid-assisted grinding was straightforward for all cocrystals,[15] as evidenced by the powder X-ray diffraction (PXRD) patterns of the products being distinct from those of the starting materials.[8,10] Exploring different stoichiometric ratios of components during grinding indicated that the cocrystals had compositions (**tp**)·(D-**ma**), (**tp**)·(DL-**ma**), (**caf**)·(D-**ma**) and (**caf**)·(DL-**ma**). That all synthesized solids were cocrystals, and not salts, was verified by solid-state CP-MAS ^{15}N NMR.[16–18]

The hydration stability of the cocrystals was assessed by exposure to relative humidity levels of 43, 75 and 98% over a period of seven days, with possible changes monitored using PXRD. In all cases the racemic cocrystal was found to be more resistant to hydration than the single-enantiomer form (Table 1). In order to qualitatively rationalise these results, we have turned to crystal structure analysis of the racemic and chiral cocrystals. Comparison of previously reported crystal structures[11] of $(\mathbf{tp})_2$·(D-**ta**) and $(\mathbf{tp})_2$·(DL-**ta**) suggests that, in this particular case, the difference in stabilities is related to the efficiency of molecular packing. The calculated density for $(\mathbf{tp})_2$·(DL-**ta**) (1.59 g cm^{-3}) is significantly higher than for its chiral analogue $(\mathbf{tp})_2$·(D-**ta**) (1.51 g cm^{-3}). This difference in packing efficiency is related to a difference in topologies of hydrogen-bonded networks in the racemic (doubly interwoven ribbons) and chiral cocrystal (triply interwoven helical chains). Since there are no significant differences in molecular conformation of **ta** between the two cocrystals, we conclude that the difference in stability of $(\mathbf{tp})_2$·(D-**ta**) and $(\mathbf{tp})_2$·(DL-**ta**) results from differences in their supramolecular architecture.

This observation made us particularly interested in the structures of chiral and racemic cocrystals (**tp**)·(D-**ma**) and (**tp**)·(DL-**ma**). The similarity of their PXRD patterns (Fig. 1) suggested isostructurality,[19] indicating that the relationship

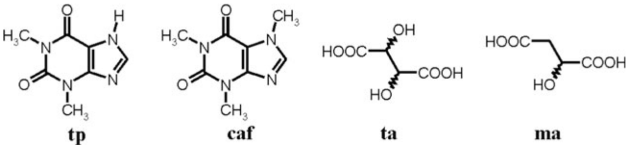

Scheme 1 Molecular diagrams of cocrystal components theophylline (**tp**), caffeine (**caf**), tartaric acid (**ta**) and malic acid (**ma**).

---

[a] *Pfizer Institute for Pharmaceutical Materials Science, Department of Chemistry, University of Cambridge, Lensfield Road, Cambridge, UK CB2 1EW. E-mail: wj10@cam.ac.uk; Fax: +44(0) 1223 336017; Tel: +44(0) 1223 336 343*
[b] *Cambridge Crystallographic Data Centre, 12 Union Road, Cambridge, UK CB2 1EZ*
[c] *School of Pharmacy, The University of Nottingham, Boots Science Building, University Park, Nottingham, UK NG7 2RD*
[d] *Department of Chemistry, University of Cambridge, Lensfield Road, Cambridge, UK CB2 1EW*

† Electronic supplementary information (ESI) available: PXRD patterns, CP-MAS NMR spectra and DSC curves; crystal structure data. See DOI: 10.1039/b717532a

Table 1 Hydration stability of chiral and racemic cocrystals[12] at different relative humidity levels over a period of up to 7 days[a]

	Relative humidity		
Cocrystal	43%	75%	98%
(caf)·**(D-ma)**	7 days	0 days	0 days
(caf)·**(DL-ma)**	7 days	7 days	0 days
(tp)$_2$·**(D-ta)**[b]	7 days	7 days	0 days
(tp)$_2$·**(DL-ta)**[b]	7 days	7 days	7 days
(tp)·**(D-ma)**	7 days	2 days	0 days
(tp)·**(DL-ma)**	7 days	7 days	7 days

[a] Numbers in each field indicate the time needed for new reflections to appear in the PXRD pattern upon exposure to a particular relative humidity level. [b] Crystal structure reported in ref. 11.

between symmetry and cocrystal stability could involve factors related to the local molecular environment. Since single crystals of **(tp)**·**(D-ma)** and **(tp)**·**(DL-ma)** could not be grown from solution, we turned to crystal structure solution using PXRD. Indexing of the **(tp)**·**(DL-ma)** PXRD pattern, and subsequent structure solution, was straightforward.[20–22] The structure is best described in terms of centrosymmetric ring-like assemblies involving two **tp** and two **ma** molecules.¶ The assemblies are held together *via* two O–H···N and two N–H···O hydrogen bonds, forming the $R_4^4(18)$ hydrogen bonding motif (Fig. 2). Adjacent assemblies stack to form layers in the crystallographic [101] plane. Determining the **(tp)**·**(D-ma)** structure was complicated by the similarity of the PXRD pattern with that of **(tp)**·**(DL-ma)**. The indexing and structure-solving procedures consistently suggested two crystallographic unit cells that were similar and centrosymmetric. Specifically, one of the solutions resembled the unit cell of **(tp)**·**(DL-ma)**, whereas the other one could be derived from it by inverting the handedness of all **ma** molecules. Since both solutions were centrosymmetric, neither could be applied to **(tp)**·**(D-ma)**. However, superposition of the two solutions revealed that the site of **ma** could be occupied by molecules of either chirality.[23] Consequently, a model structure was generated by replacing all L-molecules in the asymmetric unit of **(tp)**·**(DL-ma)** with the D-isomer, thus eliminating the centre of symmetry and doubling the number of molecules per asymmetric unit (Z').‖ The obtained structure refined well against the experimental data,[21,24] and its correctness was supported by doubling of the signals in the ^{15}N and ^{13}C CP-MAS spectra of **(tp)**·**(D-ma)**, compared to **(tp)**·**(DL-ma)** (Fig. 3), consistent with a two-fold increase in Z'.

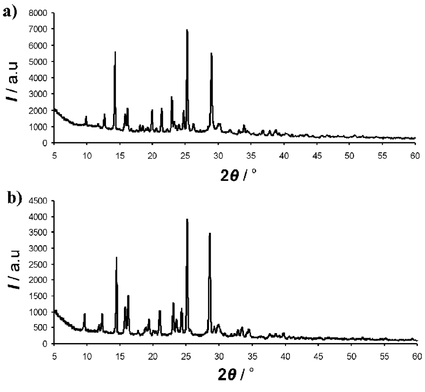

Fig. 1 PXRD patterns of: (a) **(tp)**·**(D-ma)** and (b) **(tp)**·**(DL-ma)**.

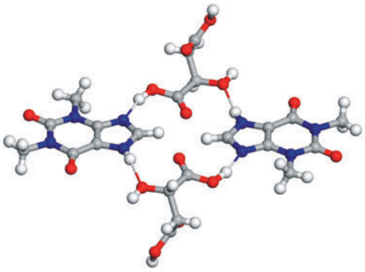

Fig. 2 A single supramolecular ring based on the $R_4^4(18)$ hydrogen bond motif in the crystal structure of **(tp)**·**(DL-ma)**.

The crystal structure of **(tp)**·**(D-ma)** reveals four-membered units held together by O–H···N and N–H···O bonds, similar to the ones observed in **(tp)**·**(DL-ma)**. In order to accommodate structural differences between **D-** and **L-ma**, one of the **ma** molecules participates in the ring using the carboxylic acid moiety linked to the CH$_2$, rather than the CHOH group. In that way, an $R_4^4(19)$ hydrogen bond motif is formed (Fig. 4a). Thus, **(tp)**·**(D-ma)** and **(tp)**·**(DL-ma)** represent an interesting case of structures having similar topologies and different connectivity.

The similarity of the overall packing arrangements in **(tp)**·**(D-ma)** and **(tp)**·**(DL-ma)** provides little explanation for the observed difference in stabilities of the two cocrystals. Indeed, the most obvious difference between the structures is not in the overall molecular arrangement, but in the molecular conformation of **ma**. The isostructurality of the two cocrystals implies that one **D-ma** molecule in the $R_4^4(19)$ motif of **(tp)**·**(D-ma)** adopts a structural role comparable to that of an **L-ma** molecule in the $R_4^4(18)$ motif of **(tp)**·**(DL-ma)**.[23] As a result, this **D-ma** molecule adopts a conformation that is $\sim$15 kJ mol^{-1} higher in energy than the corresponding molecule in **(tp)**·**(DL-ma)**.[25,26] The conformation of the other molecule of **D-ma** in **(tp)**·**(D-ma)** resembles the one in **(tp)**·**(DL-ma)** (Fig. 4b and c). Since 15 kJ mol^{-1} is a significant difference, comparable to the energy of a moderately strong hydrogen bond,[27] we suggest the conformation of **ma** as the major reason for the lower stability of **(tp)**·**(D-ma)**. Presumably, the cocrystal environment does not completely stabilise the higher energy conformation, resulting in lower stability of the cocrystal.[28] The stability difference is also observed in thermal behaviour.[29]

In summary, our results indicate that hydration stabilities of chiral and racemic cocrystals[30] may follow a trend reminiscent of Wallach's rule: the racemic cocrystal appears more stable than its chiral counterpart.[3] The structures of **tp** cocrystals studied here illustrate that the difference in stabilities can result from intermolecular (molecular packing), as well as

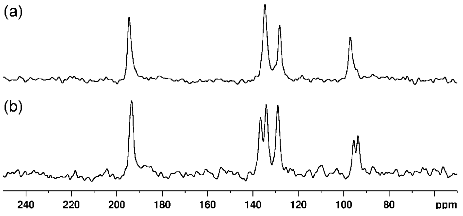

Fig. 3 ^{15}N CP-MAS spectra of: (a) **(tp)**·**(DL-ma)** and (b) **(tp)**·**(D-ma)**.

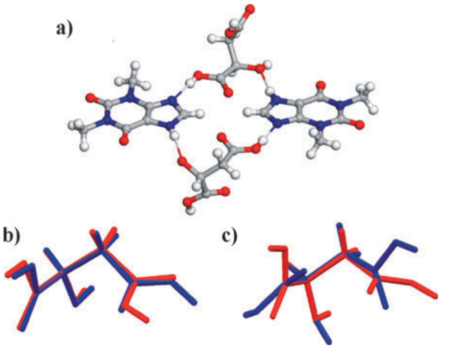

Fig. 4 (a) A single supramolecular ring in the structure of **(tp)**·(**D-ma**); overlap of an **ma** molecule in **(tp)**·(**DL-ma**) (red) with the one in **(tp)**·(**D-ma**) (blue) adopting: (b) a lower-energy and (c) a higher-energy conformation.

intramolecular (conformational strain) factors. Clearly, our results are based on a limited set of cocrystals. Nevertheless, we believe that a correlation between cocrystal symmetry and stability is attractive for cocrystal design and worth further study.§ Such a correlation would be useful when selecting between chiral or racemic cocrystal formers, and the ability to manipulate cocrystal stability through intramolecular effects provides a potential route to isostructural materials with distinct physicochemical properties. That the proposed trend extends beyond **tp** cocrystals is evidenced by the relative hydration stabilities of caffeine cocrystals **(caf)**·(**D-ma**) and **(caf)**·(**DL-ma**), as well as a previous study of thermal stability of ibuprofen cocrystals.[8] Since the structures of **(caf)**·(**D-ma**) and **(caf)**·(**DL-ma**) are still not known, the structural interpretation of the difference in their stability cannot yet be given. However, the comparison of PXRD patterns indicates it is most likely caused by crystal packing effects, similar to **(tp)**$_2$·(**D-ta**) and **(tp)**$_2$·(**DL-ta**). We are currently attempting to confirm this assumption by structure determination from PXRD. In that context, we note the successful interplay of PXRD and solid-state NMR as techniques to recognise the distinction between a cocrystal and a salt, as well as to elucidate the crystal structure of a molecular solid.

We acknowledge Drs Neil Feeder and Pete Marshall from Pfizer Global R&D for useful discussions. Financial support from Pfizer Institute for Pharmaceutical Materials Science is acknowledged.

Notes and references

‡ **D-ma** and **DL-ma** correspond to the (*S*)- and (*RS*)-forms of **ma**; **D-ta** and **DL-ta** are the (*S*,*S*)- and (*R*,*R*)(*S*,*S*)-forms of **ta**, respectively.

§ We note that, whilst hydration stabilities generally do not represent thermodynamic stabilities, it reasonable to assume that both exhibit the same qualitative trend for cocrystals within a chiral/racemic pair.

¶ **(tp)**·(**DL-ma**), ambient conditions: λ(CoKα) = 1.7889 Å, monoclinic, space group $P2_1/n$, a = 14.9568(5) Å, b = 6.0717(2) Å, c = 15.5170(5) Å, β = 106.432(2)°, χ^2 = 8.536, R_{wp} = 0.0531, R_{p} = 0.0422, $R_{\mathrm{(Bragg)}}$ = 0.0589, ρ_{calc} = 1.54 g cm^{-3}. CCDC reference number 664989.

‖ **(tp)**·(**D-ma**), ambient conditions: λ(CoKα) = 1.7889 Å, monoclinic, space group $P2_1$, a = 15.8592(7) Å, b = 6.0791(3) Å, c = 14.6549(9) Å, β = 108.589(2)°, χ^2 = 1.918, R_{wp} = 0.0583, R_{p} = 0.0457, $R_{\mathrm{(Bragg)}}$ = 0.0429, ρ_{calc} = 1.56 g cm^{-3}. CCDC reference number 664990.

1 M. J. Zaworotko, *Cryst. Growth Des.*, 2007, **7**, 4.
2 T. Friščić and L. R. MacGillivray, *Croat. Chim. Acta*, 2006, **79**, 327.
3 A. V. Trask, W. D. S. Motherwell and W. Jones, *Cryst. Growth Des.*, 2005, **5**, 1013.
4 A. N. Sokolov, T. Friščić and L. R. MacGillivray, *J. Am. Chem. Soc.*, 2006, **128**, 2806.
5 P. Vishweshwar, J. A. McMahon, J. A. Bis and M. J. Zaworotko, *J. Pharm. Sci.*, 2006, **95**, 499.
6 W. Jones, W. D. S. Motherwell and A. V. Trask, *MRS Bull.*, 2006, **31**, 875.
7 T. Friščić, D. Drab and L. R. MacGillivray, *Org. Lett.*, 2004, **6**, 4647.
8 T. Friščić and W. Jones, *Faraday Discuss.*, 2007, **136**, 167.
9 (*a*) C. P. Brock, W. B. Schweizer and J. D. Dunitz, *J. Am. Chem. Soc.*, 1991, **113**, 9811; (*b*) R. W. Lancaster, P. G. Karamertzanis, A. T. Hulme, D. A. Tocher, D. F. Covey and S. L. Price, *Chem. Commun.*, 2006, 4921.
10 (*a*) Y. Imai, N. Tajima, T. Sato and R. Kuroda, *Org. Lett.*, 2006, **8**, 2941; (*b*) E. Y. Cheung, S. J. Kitchin, K. D. M. Harris, Y. Imai, N. Tajima and R. Kuroda, *J. Am. Chem. Soc.*, 2003, **125**, 14658.
11 T. Friščić, L. Fábián, J. C. Burley, W. Jones and W. D. S. Motherwell, *Chem. Commun.*, 2006, 5009; crystallographic data for **(tp)**$_2$·(**L-ta**) and **(tp)**$_2$·(**DL-ta**) are deposited within the CSD with respective CCDC reference codes 620241 and 620242.
12 Since a racemic cocrystal of **caf** and **DL-ta** could not be obtained, the chiral cocrystal **(caf)**·(**D-ta**)[11]was not included in this study.
13 A. V. Trask, W. D. S. Motherwell and W. Jones, *Int. J. Pharm.*, 2006, **320**, 114.
14 N. Shan, F. Toda and W. Jones, *Chem. Commun.*, 2002, 2372.
15 Pure samples of **(caf)**·(**DL-ma**) were prepared by liquid-assisted grinding of enantiomeric cocrystals[11] **(caf)**·(**L-ma**) and **(caf)**·(**D-ma**).
16 The chemical shift of the **tp** or **caf** imidazole nitrogen atom was between 194 and 195 ppm (relative to ammonium at 0 ppm) in all cases, showing it to be non-protonated.[17] For comparison, corresponding shifts in **caf** benzenesulfonate salt and the cocrystal of **caf** with adipic acid are 134 ppm and 193 ppm, respectively.
17 For assignment of solid-state ^{15}N and ^{13}C spectra of **caf**, see: J. Sitkowski, L. Stefaniak, L. Nicol, M. L. Martin, G. J. Martin and G. A. Webb, *Spectrochim. Acta, Part A*, 1995, **51**, 839.
18 Z. Li, Y. Abramov, J. Bordner, J. Leonard, A. Medek and A. V. Trask, *J. Am. Chem. Soc.*, 2006, **128**, 8199.
19 L. Fábián and A. Kálmán, *Acta Crystallogr., Sect. B: Struct. Sci.*, 1999, **55**, 1099.
20 W. I. P. David, K. Shankland, J. van de Streek, E. Pidcock, W. D. S. Motherwell and J. C. Cole, *J. Appl. Crystallogr.*, 2006, **39**, 910.
21 PXRD data for structure solution was collected using CoKα radiation.
22 PXRD revealed small amounts of **tp** (0.5 mol %) and **DL-ma** (6.5 mol %) impurities in samples of **(tp)**·(**DL-ma**), regardless of the preparation method. These were included in the Rietveld refinement.
23 J. van Mil, L. Addadi, M. Lahav and L. Leiserowitz, *J. Chem. Soc., Chem. Commun.*, 1982, 584.
24 The non-centrosymmetric structure is supported by very weak reflections in the PXRD pattern that would be systematically absent in the centrosymmetric case.
25 Preliminary single-point energy calculations were done using the GAMESS(US) program[26] B3LYP/6-31G(d) method, and provided 14.64 kJ mol^{-1} as the energy difference between the conformations.
26 M. W. Schmidt, K. K. Baldridge, J. A. Boatz, S. T. Elbert, M. S. Gordon, J. H. Jensen, S. Koseki, N. Matsunaga, K. A. Nguyen, S. Su, T. L. Windus, M. Dupuis and J. A. Montgomery, *J. Comput. Chem.*, 1993, **14**, 1347.
27 T. Steiner, *Angew. Chem., Int. Ed.*, 2002, **41**, 48.
28 Small differences in hydrogen-bonded structures of **(tp)**·(**D-ma**) and **(tp)**·(**DL-ma**) are mutually compensated and are probably of minor significance for cocrystal stability. For example, the shortening of N–H···O bonds in the ring motif of **(tp)**·(**D-ma**) is likely to be compensated by concomitant lengthening of O–H···N bonds.
29 **(tp)**·(**D-ma**) melts at 135 °C and **(tp)**·(**DL-ma**) at 170 °C, with respective enthalpies of fusion being −30.4 and −44.1 kJ mol^{-1}. The melting point of the **(tp)**·(**D-ma**) and **(tp)**·(**L-ma**) conglomerate was calculated to be 105 °C, using the simplified Schröder–van Laar equation[9a].
30 Decomposition of a multi-component racemic solid into a conglomerate has also been observed; see: K. Yoshizawa, S. Toyota and F. Toda, *Chem. Commun.*, 2004, 1844.